Planta (2010) 232:987–997
DOI 10.1007/s00425-010-1232-8

ORIGINAL ARTICLE

Cloning and molecular characterization of a glycerol-3-phosphate *O*-acyltransferase (GPAT) gene from *Echium* (Boraginaceae) involved in the biosynthesis of cutin polyesters

Aurora Mañas-Fernández · Yonghua Li-Beisson · Diego López Alonso · Federico García-Maroto

Received: 7 June 2010 / Accepted: 23 June 2010 / Published online: 25 July 2010

Abstract The glycerol-based lipid polyester called cutin is a main component of cuticle, the protective interface of aerial plant organs also controlling compound exchange with the environment. Though recent progress towards understanding of cutin biosynthesis has been made in *Arabidopsis thaliana*, little is known in other plants. One key step in this process is the acyl transfer reaction to the glycerol backbone. Here we report the cloning and molecular characterization of *EpGPAT1*, a gene encoding a glycerol-3-phosphate *O*-acyltransferase (GPAT) from *Echium pitardii* (Boraginaceae) with high similarity to the *AtGPAT4*/*AtGPAT8* of *Arabidopsis*. Quantitative analysis by qRT-PCR showed highest expression of *EpGPAT1* in seeds, roots, young leaves and flowers. Acyltransferase activity of EpGPAT1 was evidenced by heterologous expression in yeast. Ectopic expression in leaves of tobacco plants lead to an increase of C16 and C18 hydroxyacids and α,ω-diacids in the cell wall fraction, indicating a role in the biosynthesis of polyesters. Analysis of the genomic organization in *Echium* revealed the presence of *EpGPAT2*, a closely related gene which was found to be mostly expressed in developing leaves and flowers. The presence of a conserved HAD-like domain at the N-terminal moiety of GPATs from *Echium*, *Arabidopsis* and other plant species suggests a possible phosphohydrolase activity in addition to the reported acyltransferase activity. Evolutive implications of this finding are discussed.

Keywords Acyltransferase · Cuticle biosynthesis · Cutin · *Echium* · GPAT · Lipid polyesters

Abbreviations

AT	Acyltransferase
BSTFA	*N*,*O*-bis(trimethylsilyl)trifluoroacetamide
CaMV	Cauliflower mosaic virus
CSPD	Disodium 3-(4-methoxyspiro {1,2-dioxetane-3, 2′-(5′-chloro)tricyclo [3.3.1.13,7]decan}-4-yl)phenyl phosphate
CTAB	Cetyl trimethyl ammonium bromide
DIG	Digoxigenin
DTNB	5, 5′-Dithio-bis(2-nitrobenzoic acid)
EtBr	Ethidium bromide
GC	Gas-liquid chromatography
G3P	Glycerol-3-phosphate
GPAT	Glycerol-3-phosphate *O*-acyltransferase
HAD	Haloacid dehalogenase
qPCR	Quantitative PCR
RACE	Rapid amplification of cDNA ends

Introduction

The cuticle is a complex hydrophobic layer that covers the epidermis of aerial organs in land plants (Kolattukudy 2001;

Electronic supplementary material The online version of this article (doi:10.1007/s00425-010-1232-8) contains supplementary material, which is available to authorized users.

A. Mañas-Fernández · D. L. Alonso · F. García-Maroto (✉)
Universidad de Almería, Grupo de Biotecnología de Productos Naturales (BIO-279), 04120 Almería, Spain
e-mail: fgmaroto@ual.es

Y. Li-Beisson
Department of Plant Biology and Environmental Microbiology, CEA-CNRS-Université Aix Marseille, CEA Cadarache, 13108 Saint Paul lez Durance, France

Present Address:
A. Mañas-Fernández
Department of Botany, University of British Columbia, 6270 University Blvd, Vancouver, BC V6T 1Z4, Canada

Nawrath 2002; Kunst et al. 2004; Pollard et al. 2008). This structure constitutes an extracellular barrier that limits air and water/solute exchange and also provides protection against UV radiation and pathogen challenges. The cuticle is composed of a lipophilic polymer matrix embedded with wax lipids (Kunst and Samuels 2003). Partial depolymerization of the cuticle matrix can be achieved by cleaving the ester bonds from the polyester fraction called cutin, while the remaining non-hydrolysable fraction corresponds to the poorly known component called cutan. Cutin is predominantly built from C_{16} and C_{18} aliphatic chains that are linked by ester bonds, typically between carboxy and ω-hydroxy groups of individual fatty acids derivatives (Kolattukudy 2001). ω-Hydroxyacids with additional hydroxy and epoxy groups at internal positions (mid-chain usually) are among the major products obtained after depolymerization. Unusual composition is found in some plants like *Arabidopsis*, where α,ω-dicarboxylic acids are the main cutin monomers of leaves and stems (Bonaventure et al. 2004; Franke et al. 2005).

Despite its importance, the structure and biosynthesis of plant polyesters has remained relatively unknown for a long time. Nevertheless, a great progress has been made in the last 5 years in the elucidation of the biochemical pathways leading to the synthesis of cutin and the related polyester suberin (Franke and Schreiber 2007; Pollard et al. 2008) in the model plant *A. thaliana* (Li-Beisson et al. 2010). Central to the biosynthetic pathway is esterification of glycerol-3-phosphate, catalyzed by a glycerol-3-phosphate *O*-acyltransferase (GPAT) activity (Pollard et al. 2008). A group of eight genes (*AtGPAT1* to *AtGPAT8*) encoding putative GPATs were identified in *A. thaliana*, mainly based on the presence of conserved motifs found in similar acyltransferases from bacteria, yeast and mammals (Zheng et al. 2003; Beisson et al. 2007). Five of these genes (*AtGPAT1*, *AtGPAT4*, *AtGPAT5*, *AtGPAT6*, and *AtGPAT7*) encoded proteins with detectable GPAT activity when assayed by heterologous expression in crude yeast fractions using acyl-CoAs and glycerol-3-phosphate as substrates (Zheng et al. 2003). One member, *AtGPAT1*, encodes a mitochondrial isozyme that is necessary for pollen development, but its deficiency does not affect the seed oil content (Zheng et al. 2003). All other characterized members of this family (*AtGPAT4*, *AtGPAT5*, *AtGPAT6*, and *AtGPAT8*) were found to be involved in the biosynthesis of the protective polyesters suberin and cutin, rather than in the building of membrane or reserve glycerolipids (Beisson et al. 2007; Li et al. 2007a, b; Li-Beisson et al. 2009). Analysis of loss-of-function mutants in *Arabidopsis* demonstrated an essential role of *AtGPAT5* for suberin biosynthesis in the root and seed coat (Beisson et al. 2007). Similarly, *AtGPAT4* and *AtGPAT8* have been shown to encode likely redundant or overlapping activities necessary for the assembly of cutin monomers in stems and leaves (Li et al. 2007a), whereas *AtGPAT6* is involved in cutin assembly in flowers (Li-Beisson et al. 2009). Numerous evidences indicate a central role for glycerol and its acylation reaction in the synthesis of suberin and cutin polymers. Monomer composition analysis (Moire et al. 1999; Graça and Pereira 2000; Graça et al. 2002) and overexpression of *AtGPAT5* in *Arabidopsis* and tobacco plants which lead to secretion of monoacylglycerols (MAGs) onto leaf surface (Li et al. 2007b) thus indicated it. However, little is known about the exact nature of GPAT acyl-substrates, and the sequence of reactions leading to the final synthesis and assembly of the glycerol-lipid based polyesters (Pollard et al. 2008).

As stated above, a role in polyester biosynthesis has been demonstrated in *Arabidopsis* for four GPAT enzymes. No homologs of these *Arabidopsis* GPATs have been characterized in other plant species, however. Besides, in species accumulating hydroxy fatty acids (or more generally unusual fatty acids) in seed oils, it is possible that polyester-type GPAT acyltransferases also play a role in oil synthesis (Li and Beisson 2009). This hypothesis is supported by the fact that some unusual fatty acids are found in both polyesters and seed oils, and by the observation that several enzymes of unusual fatty acid synthesis are divergent forms of enzymes of normal fatty acid synthesis. A number of molecular studies on lipid biosynthesis have been performed in *Echium* plants (García-Maroto et al. 2002; Mañas-Fernández et al. 2009) which are characterized by the accumulation of unusual Δ^6-desaturated fatty acids (γ-linolenic and stearidonic acids) in the seed oil. Here, we report on the cloning and molecular characterization of *EpGPAT1*, a homolog of *Arabidopsis* polyester-type GPATs which was isolated from the seeds of *Echium pitardii* (Boraginaceae). Over-expression of *EpGPAT1* in tobacco revealed that this gene plays a role in the metabolism of the ω-oxidized fatty acids constitutive of polyesters.

Materials and methods

Biological material

Seeds of *Echium pitardii* A. Chev. ex D. Bramwell (=*E. lancerottense* Lems et Holz) were originally collected from plants located in their natural habitat at Lanzarote (Canary Islands) and further reproduced in the lab. Seedlings (6–8 leaves stage) were grown at 25°C, under the controlled conditions of growth cabinets with a 16 h light/8 h dark photoperiod and 70% relative humidity. Leaf material from seedlings was used as a DNA source, while the different tissues of *E. pitardii* utilized for RNA extraction and

Northern-blot analysis were sampled from mature plants cultivated in the greenhouse. Tobacco plants *Nicotiana tabacum* L. var. Wisconsin-38 (Lehle Seeds, Round Rock, TX, USA), grown as indicated before, were used for *Agrobacterium* stable transformation experiments. The wild-type yeast strain INVSc1 (Invitrogen, Carlsbad, CA, USA), and the *gat1Δ* mutant strain (BY4742, *MATα*, *his3Δ1*, *leu2Δ0*, *lys2Δ0*, *ura3Δ0*, *YKR067w::kanMX4*) from the EUROSCARF collection (http://web.uni-frankfurt.de/fb15/mikro/euroscarf/) were used to assay GPAT activity by heterologous expression.

Cloning of *Echium GPAT* genes

EpGPAT1 gene was cloned by RT-PCR amplification of a partial cDNA using degenerated primers, followed by 3′ and 5′-RACE to complete the flanking sequences. Briefly, an oligo-dT primed cDNA was synthesized from ca. 1 μg of total RNA obtained from developing fruits (seeds) of *E. pitardii* by employing the SuperScript® III First-Strand Synthesis System for RT-PCR kit (Invitrogen) following the manufacturer's instructions. Initial RT-PCR amplification on the cDNA was done using two sets of degenerated oligonucleotide primers (EGPAT1/2 and EGPAT3/4) designed against the GPAT conserved motifs VVCPEGTTCREP and GFECTNLTRRDK (see Supplementary Fig. 1). RACE amplification was performed with the SMART® RACE cDNA Amplification Kit (Clontech, Mountain View, CA, USA) employing nested pairs of gene-specific primers. Finally, a whole cDNA was obtained by RT-PCR as described before, using the flanking primers EGPAT-Up (5′-TTAAGAGCTCACCATGGCTCTGCCTAAGCCTGAAATAC-3′) and EGPAT-Down (5′-TCTATCTAGATCACTTCTTTGAATACATTGATTCAACC-3′) containing suitable restriction sites. A proof-reading DNA polymerase Accuprime® (Invitrogen) and buffer I provided by the manufacturer were used in the amplification. The PCR fragment was sub-cloned into the pGEM®-T Easy vector (Promega, Madison, WI, USA) after A addition and several clones were fully sequenced allowing detection of two variants (*EpGPAT1-1* and *EpGPAT1-2*) of the gene (see Results for further explanation). DNA clones were sequenced on both strands using a Perkin-Elmer ABI-310 DNA automated sequencer, and the BigDye® Terminator v3.1 chemistry. The cDNA for *EpGPAT2* was obtained by RT-PCR on developing flower total RNA using the above primers EGPAT-Up and EGPAT-Down.

cDNA sequences were deposited in the GenBank under the accession numbers HM241742, HM241743, HM241744 for *EpGPAT1-1*, *EpGPAT1-2*, and *EpGPAT2*, respectively.

Cladistic analysis

GPAT-related amino acid sequences were aligned using the program ClustalX v.2 (http://www.clustal.org/) under the default settings, and further refined by visual inspection. The alignment output was used to generate a phylogenetic tree based on the Minimum Evolution method (Rzhetsky and Nei 1992), as implemented in the MEGA package v4.0.2 (Tamura et al. 2007). The Poisson correction metric was used together with the pairwise deletion option, and confidence of the tree branches was checked by bootstrap generated from 1,000 replicates. Rooting of the tree was accomplished by using plastidial GPAT sequences as outgroup. For sequences selected in Fig. 1, the alignment was visualized using the Boxshade v. 3.21 software (http://www.ch.embnet.org/software/BOX_form.html).

Nucleic acids isolation and Southern-blot analysis

Genomic DNA was isolated from *Echium* seedlings by a CTAB-based extraction procedure (Taylor and Powel 1982). DNA (ca. 5 μg) was restricted with the appropriate restriction enzymes, separated on a 0.8% agarose gel, and transferred by capillarity onto Hybond®-N^+ nylon membranes (Amersham, Little Chalfont, UK). Filters were UV-crosslinked, pre-hybridized at 42°C for 5 h in the 50% formamide/high SDS buffer recommended by the DIG manufacturer (Roche Diagnostics, Indianapolis, IN, USA), and hybridized at the same temperature and same buffer solution (stringent conditions), containing any of the digoxigenin-labeled probes (probe 1 or probe 2; Supplementary Fig. 3) for *EpGPAT1*. High stringency washes were performed twice at 65°C during 15 min in buffer containing 0.1× SSC, 0.1% SDS, and the luminogenic substrate CSPD® was used for detection, following the instructions provided with the DIG detection kit. Chemiluminescence images were registered using a Chemie Genius2 detection system (Syngene, Beacon House, Nuffield Road, Cambridge, UK). The *GPAT* probes were obtained from the cDNA clone following a random primed labeling procedure designed for DIG probes (Roche Diagnostics).

Total RNA was extracted from different tissues of *E. pitardii* plants, using the method described by Chang et al. (1993) with minor modifications. Composition of the extraction buffer was modified so that polyvinyl pyrrolidone and spermidine were replaced by the RNase inhibitors *p*-aminosalicilic acid (20 mg/ml) and sodium naftalensulfonate (5 mg/ml).

Quantitative and semi-quantitative PCR

EpGPAT1 mRNA, and 18S ribosomal RNA (rRNA) expression were determined by quantitative RT-PCR using Taqman MGB® (Life Tecnologies, Carlsbad, CA, USA) specific probes and the ABI7000 Sequence Detection System® (Applied Biosystems, Foster City, CA, USA). Sequences were designed with Primer Express® software (Applied Biosystems) for the *EpGPAT1* gene-specific primers and fluorescent (VIC-labeled) hybridization probe as follows: forward primer 5′-GGAAGGTGGTGGT TACTGCAAAT-3′; reverse primer, 5′ ATTCACCTCA ATCTCTGTTCCAA-3′; and probe, 5′-TGAGCCATTT GTGAGGGATTATTTGGG-3′. Amplification was carried out on cDNA synthesized as indicated above, after RNA digestion with RQ1 RNase-Free DNase (Promega) to eliminate contaminating genomic DNA. The TaqMan Core Reagent Kit (Life Technologies) was used for PCR, following the standard protocol provided by the manufacturer. Relative gene expression was determined using the comparative Ct method (ΔΔCt) (Livak and Schmittgen 2001), and the constitutive 18S rRNA as an endogenous control. A validation of the quantitation method was performed in a seriated template dilution experiment, and similar efficiencies were obtained for the *EpGPAT1* target and the 18S rRNA standard. PCR products were analyzed by agarose gel electrophoresis and showed the expected size (ca. 140 bp) for the amplicon. The mean value of five replicas was calculated besides the experimental error: $2^{-(\Delta\Delta Ct \pm SDt)}$, where the total standard deviation (SDt) was calculated from the SD of each gene.

For semi-quantitative PCR, random primer-directed cDNA was synthesized from 2 μg of total RNA as described above, and 400 ng of the cDNA was amplified in a 40 μl reaction volume using 0.8 units of iProof High-Fidelity DNA Polymerase (BioRad, Hercules, CA, USA). The PCR program comprised a denaturation step of 30 s at 98°C and 17–25 cycles of 10 s at 98°C, 20 s at 59°C, 15 s at 72°C. Gene-specific primers were designed to amplify the same cDNA region (spanning a putative intron) as follows: sqRT1-F-(5′-CCACTCAATTGCAGCTGATTTG-3′) and sqRT1-R (5′-TTTCCTCTTGCATTTCTCAAACACTTT -3′) for *EpGPAT1*, and sqRT2-F (5′-CCACCGCTCCG TAGCGGCGGACCTC-3′) and sqRT2-R (5′-CTTCCTC TCACATTTATCAAACACCTC-3′) for *EpGPAT2*. Amplification for the rRNA18S was used as a constitutive control to check for equal template loading. cDNA amounts and the number of cycles (25 cycles for *EpGPAT* genes and 17 cycles for the rRNA18S) were experimentally determined to be non-saturating. The identity of the PCR fragments was confirmed by direct sequencing.

Heterologous yeast expression and determination of GPAT activity

The whole coding sequence from the two allelic variants *EpGPAT1-1* and *EpGPAT1-2* was transcriptionally fused to the *GAL1* inducible promoter of the pYES2 expression vector (Stratagene, La Jolla, CA, USA), by cloning into the *Sac*I/*Eco*RI restriction sites. The resulting plasmids were used to transform *Saccharomyces cerevisiae* (*gat1Δ*) according to the LiAcO method (Elble 1992). Cultures were grown at 28°C in standard minimal medium supplemented with the auxotrophic requirement of the strain plus 1% (w/v) raffinose, and expression was further induced on a 0.4 OD_{600} culture by the addition of galactose 2% (w/v) plus 1% (w/v) raffinose. Incubation under inductive conditions was prolonged for 8 h at the same temperature. Yeast cells were collected by centrifugation, further washed with 1.3% NaCl, and stored at −70°C until use.

Yeast homogenates were prepared with glass beads by standard protocols in lysis buffer (50 mM Hepes, pH 7.0, 2 mM EDTA, 10% glycerol). Large cell debris was spun at 1,500 *g*, 4°C, for 5 min. The supernatant was then centrifuged at 20,000 *g*, 4°C, for 30 min, and the sediment was gently resuspended in sodium phosphate buffer 100 mM pH 7.0, aliquoted and stored at −70°C until assay. GPAT activity was determined by the DTNB method (Bafor et al. 1990), using commercial oleoyl-CoA (Sigma-Aldrich, St Louis, MO, USA) as the acyl donor. After optimization of the different components, the reaction was carried out at 25°C in a 400 μl volume containing sodium phosphate 100 mM pH 7.0, 5 mM EDTA, 1 mg/ml BSA, 0.12 mM DTNB, 1 mM G3P, and 50–210 μg of the protein fraction. The reaction was started by adding oleoyl-CoA to a final concentration of 62.5 μM, and absorbance at 405 nm was recorded for 2 min after a 30–60 s lag. Specific activities were expressed as μmol of released CoA per min and mg of protein extract. Protein concentrations in the extracts were estimated by the Bradford (1976) method using bovine serum albumin as a standard.

Tobacco transformation and lipid analysis

Overexpression of *EpGPAT1* in tobacco plants was carried out by cloning of the whole coding sequences (cDNAs) from the two allelic variants of the gene into the pJIT60 vector (Guerineau 1995), under the control of the double 35S-CaMV promoter and the termination/polyadenylation signals from the same gene. The resulting cassette was liberated by digestion with appropriate restriction enzymes and sub-cloned into the pBIN19 vector (Bevan 1984). Plasmid constructs were introduced into *Agrobacterium*

tumefaciens LBA4404 cells and then used for tobacco leaf disk transformation, essentially as described by Horsch et al. (1985), using kanamycin resistance as selection marker. Plants transformed with the empty vector (6 lines) were used as a negative control. Primary transgenic plants were checked by Northern-blot analysis on leaf total RNA, as described above. Selected lines were selfed, and lipid analysis performed on leaves from pools of progeny plants (T_1) selected by kanamycin resistance and grown to a 8–10 developed leaves stage.

Fatty acid composition of tobacco leaves was analyzed after acidic transmethylation as published elsewhere (Rodriguez-Ruiz et al. 1998).

Analysis of cuticular waxes was performed as follows. Leaves were dipped in dichloromethane for 30 s, the solvent evaporated under a stream of N_2 gas, and *n*-octacosane used as internal standard. The waxes were derivatized by heating at 110°C for 10 min in pyridine:BSTFA (1:1, v/v). The silylated samples were analyzed by GC using an Agilent Technologies 6890N equipment (Agilent Technologies, Santa Clara, CA, USA) with an Omegawax TM 250 (Supelco) capillary column (30 m × 0.25 mm i.d., 0.25 μm film thickness). Molecular identification was performed using an Agilent 7890 series gas chromatograph (Agilent Technologies) interfaced to an Agilent 5975 mass selective detector (MSD). Leaf areas were determined by blotting on filter paper after wax extraction and image scanning using a Syngene® ChemiGenius Imager. For polyester analysis, the NaOMe depolymerization and GC–MS analysis method was performed on fully delipidated leaves as described before (Molina et al. 2006). Cutin monomers are expressed on a leaf surface basis.

Results

Cloning and characterization of a *GPAT*-related gene from *Echium*

A search for genes encoding putative glycerol-3-phosphate acyltransferases (GPAT) was performed in *Echium* by RT-PCR, using different sets of degenerated oligonucleotide primers. These primers were directed against two highly conserved motives identified in a group of proteins from *Arabidopsis* for which GPAT activity was reported (Zheng et al. 2003; Beisson et al. 2007) (Supplementary Fig. 1). Amplification on the cDNA from developing *Echium* seeds consistently rendered the same product, even though the primers were potentially able to amplify any of the eight *AtGPAT* genes initially described in *Arabidopsis* (Supplementary Fig. 1). The partial sequence corresponding to the PCR fragment (about 350 bp) was further completed by 3′ and 5′ RACE (see "Materials and methods") and a whole cDNA was finally obtained using appropriate flanking primers. Two slightly different clones were detected differing by eight nucleotide positions in the coding region, probably representing allelic variants. Only one of the changes produced amino acid replacement, with either Ala or Thr at position 224 (accession numbers HM241742 and HM241743, Fig. 1), and the two genes were designated *EpGPAT1-1* and *EpGPAT1-2*, respectively.

The protein encoded by *EpGPAT1* comprises 503 residues, with a molecular mass of 56,294 Da and an isoelectric point of 9.36. Software analysis supports the lack of a signal peptide and the presence of two transmembrane domains (Fig. 1). A bipartite domain structure can be recognized in EpGPAT1 (Fig. 1). The typical acyltransferase (AT) domain containing the four conserved boxes (AT-I to AT-IV) (Lewin et al. 1999) is localized within the C-terminal half of the molecule. Catalytic residues histidine and aspartic in AT-I, glycine in AT-III, and a proline in AT-IV are all present in EpGPAT1, as well as the arginine (AT-II), glutamic (AT-III) and serine (AT-III) residues involved in the binding to the G3P substrate (Fig. 1). Besides the AT region, a haloacid dehalogenase (HAD)-like domain (CDD database cl11391), can be recognized at the N-terminal half of EpGPAT1. This conserved domain is present in a superfamily of proteins, mainly including phosphohydrolases. A close inspection of this region in EpGPAT1 and putative orthologues reveals the presence of the highly conserved motifs (HAD-I to HAD-IV, Fig. 1) described in HAD-like proteins (Burroughs et al. 2006). They include the typical DXD signature containing the critical Asp residue acting as nucleophile in the reaction, the extremely conserved Thr and Lys in HAD-II and HAD-III boxes, respectively, both contributing to the stability of the reaction intermediates, and a GDXXXD motif in HAT-IV containing the acidic residues required for coordination to the Mg^{2+} ion in the active site.

A BLASTP search in the GenBank using EpGPAT1 as entry reveals the presence of putative orthologues in other organisms. High similarities (79–81% identical residues, 89–90% similarity) are found for proteins annotated as putative glycerol-3-phosphate acyltransferases of *Vernicia fordii*, *Populus trichocarpa*, *Ricinus communis* and *Vitis vinifera*, among others (Fig. 1). In *A. thaliana*, EpGPAT1 is most similar to AtGPAT4 (75% identity, 88% similarity), and AtGPAT8 (75% identity, 86% similarity), two proteins which have been involved in the synthesis of cutin polymers (Li et al. 2007a). A cladistic analysis using the Minimum Evolution methodology (Rzhetsky and Nei 1992) groups EpGPAT1 in the same clade of AtGPAT4/8, sister to the group of AtGPAT6 (Fig. 2). In this analysis, other members of the AtGPAT family lie apart from the EpGPAT1 group. Highly similar proteins

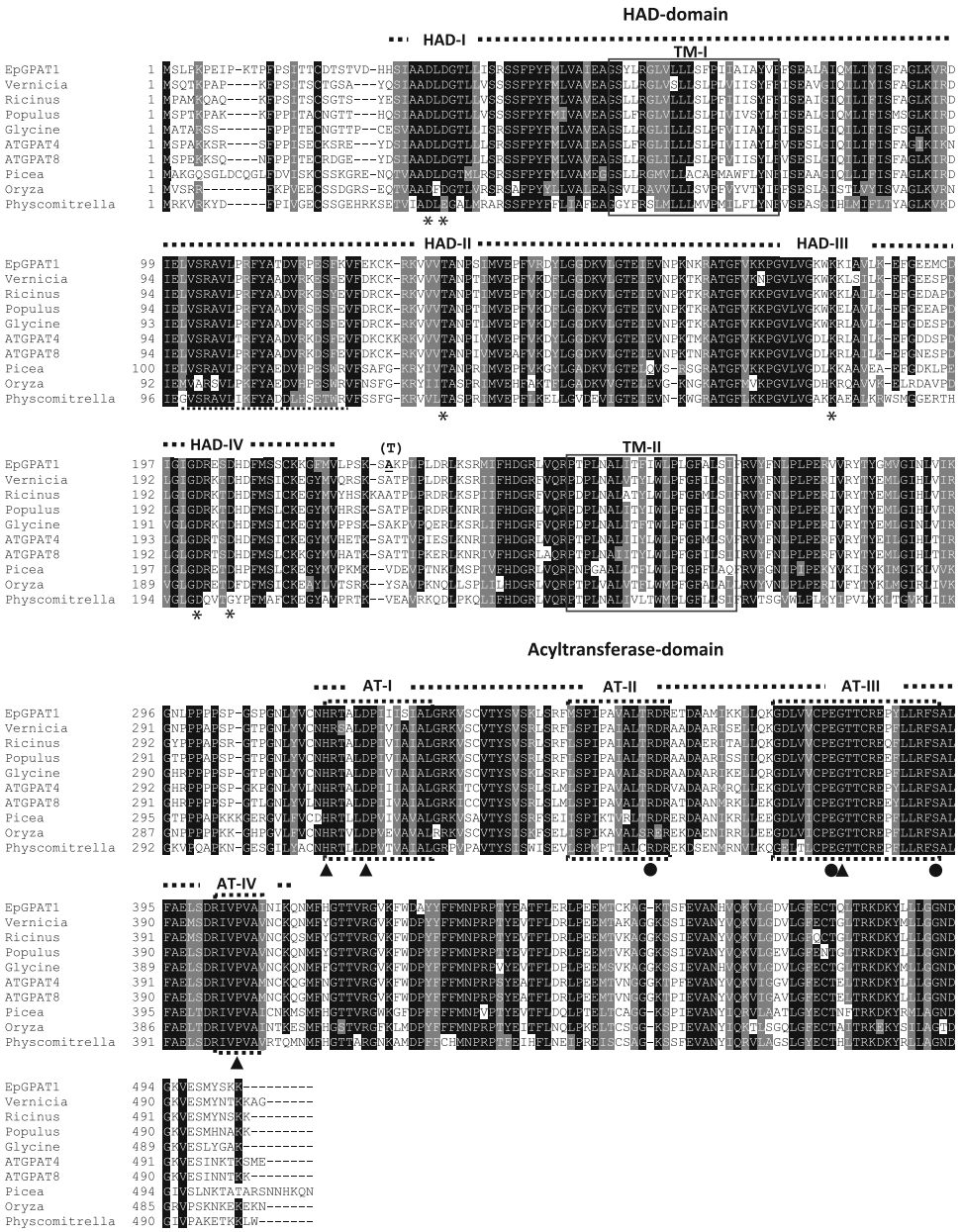

Fig. 1 Amino acid alignment of EpGPAT1 and closely related proteins found in the GenBank. Putative orthologues from *Vernicia fordii* (*ACT32032*), *Ricinus communis* (*XP_002511873*), *Populus trichocarpa* (*XP_002320138*), *Glycine max* (*AK244277*), *Picea sitchensis* (*ABK25381*), *Oryza sativa* (*NP_001044839*) and *Physcomitrella patens* (*XP_001771186*) besides AtGPAT4 (*NP_171667*) and AtGPAT8 (*NP_191950*) from *A. thaliana* were aligned using the ClustalX v2.0 software (http://www.clustal.org/), and similarities highlighted with the Boxshade program (http://www.ch.embnet.org/software/BOX_doc.html). Residues shared by a fraction of sequences above 0.9 are shaded, identical residues in *black*, similar residues in *grey*. Two putative transmembrane domains TMI and TMII predicted by TMPRED (http://www.ch.embnet.org/software/TMPRED_form.html) are boxed with *solid lines*. HAD-like and acyltransferase domains are marked by doted lines, besides characteristic motifs, AT-I to AT-IV and, HAD-I to HAD-IV, for the acyltransferase and HAD domains, respectively. Critical residues previously identified in similar proteins are marked by *asterisks* (HAD domain), *dots* (binding site in AT domain) or *triangles* (catalytic residues in AT domain). The presence of either Ala or Thr (T) at position 224 of the EpGPAT1 variants (see the text) is indicated

to EpGPAT1 are also found in monocots like *Oryza*, gymnosperms like *Picea*, and even in the moss *Physcomitrella patens* (54% identity, 71% similarity) were not only critical residues are present but also long identity stretches, thus revealing a strong conservation of this protein within the plant kingdom (Fig. 1). Outside the

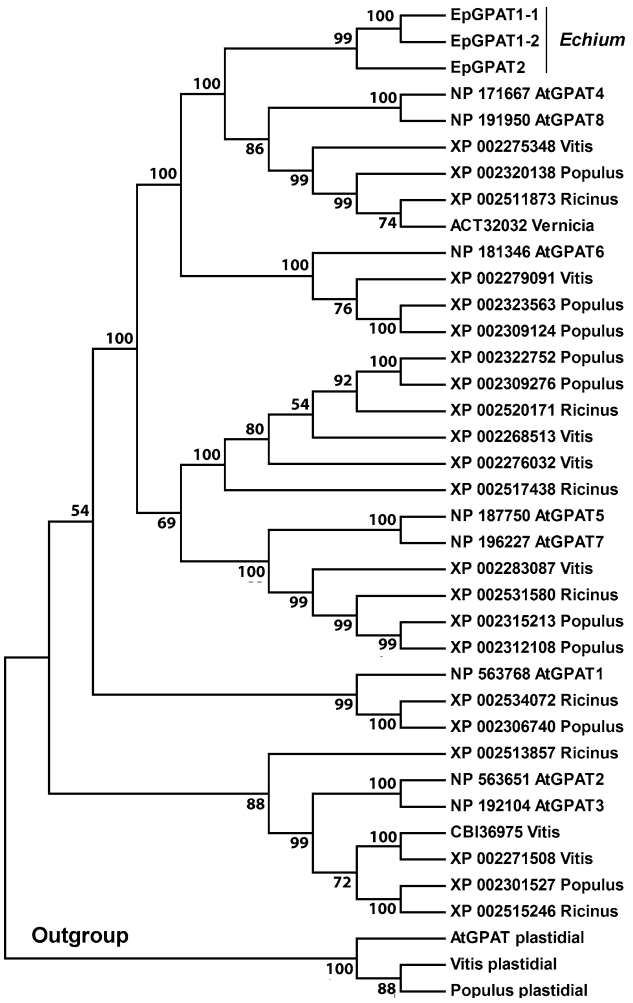

Fig. 2 Minimum evolution tree depicting relationships among *Echium* GPATs and related proteins from dicot species. Amino acid sequences retrieved from the GenBank (accession numbers provided) were aligned and further analyzed using the MEGA software v4 (Tamura et al. 2007) as described in "Materials and methods". Plastidial GPATs are used as the outgroup. Bootstrap values supporting the different clades are indicated on the nodes

plant kingdom, the highest similarity to EpGPAT1 was found for HAD-like phosphohydrolases of bacteria sharing 47–49% similar residues in the HAD domain (Supplementary Fig. 2).

Genomic organization and expression analysis of *EpGPAT1*

Genomic organization of *EpGPAT1* in *Echium* was investigated by Southern-blot analysis. Patterns obtained after digestion of genomic DNA with several restriction enzymes reveal several hybridizing bands, using either of two different cDNA derived probes under stringent conditions (Supplementary Fig. 3). Though accurate interpretation of these patterns is obscured by the presence of three presumable introns (deduced by comparison with the putative orthologues AtGPAT4/8 from *Arabidopsis*), the appearance of a minimum of two bands in the hybridization with probe 2 (which does not span intronic regions), suggests the presence of at least two highly related genes in the *Echium* genome. This finding prompted us to investigate the presence of sequences related to *EpGPAT1* by RT-PCR on RNA extracted from non-seed tissues. Interestingly, a cDNA clone (acc. no. HM241744) was obtained from developing flowers with a high similarity to *EpGPAT1*. The protein encoded by this gene, named *EpGPAT2*, shows 98.5% of similar residues (89.3% identity) to EpGPAT1 (Supplementary Fig. 4), and appears as sister to EpGPAT1 in cladistic analysis (Fig. 2).

The expression pattern in different organs of the *Echium* plant was investigated for the two *EpGPAT* genes by semi-quantitative RT-PCR using gene-specific primers (Fig. 3a). The highest expression for *EpGPAT1* was found in roots, developing leaves, fruits and flowers. Relatively low expression was detected in stem and mature leaves. For *EpGPAT2*, relatively high expression was found in young leaves and flowers, while a much lower amplification was obtained in plant roots, conversely to what it was found for *EpGPAT1*. Again, low expression in mature leaves was recorded compared to the developing stage. The expression pattern for *EpGPAT1* was confirmed by qPCR using a gene-specific Taqman probe (MGB®, Applied Biosystems) (Fig. 3b). These results are also in agreement to Northern-blot analysis, though in this case hybridisation could not distinguish among the two highly similar *EpGPAT* genes (results not shown).

Investigation on the activity of EpGPAT1

Complementation assays using *plsB* mutants of *Escherichia coli* (SJ22 and BB26-36) defective in GPAT activity failed to rescue the mutation when the *EpGPAT1* gene was overexpressed (results not shown). To overcome limitations of the prokaryotic system, the activity of the *EpGPAT1* product was also assayed by heterelogous expression in the yeast mutant *gat1Δ* (Y15983). This mutant strain harbors a mutation in the *GAT1* gene that encodes the major ER-bound GPAT. Since this mutant has a very low GPAT activity, it has been used to test functionality of putative GPATs (Zheng and Zou 2001). The coding sequences (cDNAs) for the two variants of the gene *EpGPAT1-1* and *EpGPAT1-2* were cloned in the pYES2 expression vector under the control of the galactose-inducible promoter of *GAL1*. It has been described that most of the GPAT activity in yeast is present in the fraction containing mitochondria and heavy microsomes (Zinser et al. 1991), with the higher specific activity corresponding to lipid particles associated to these organelles

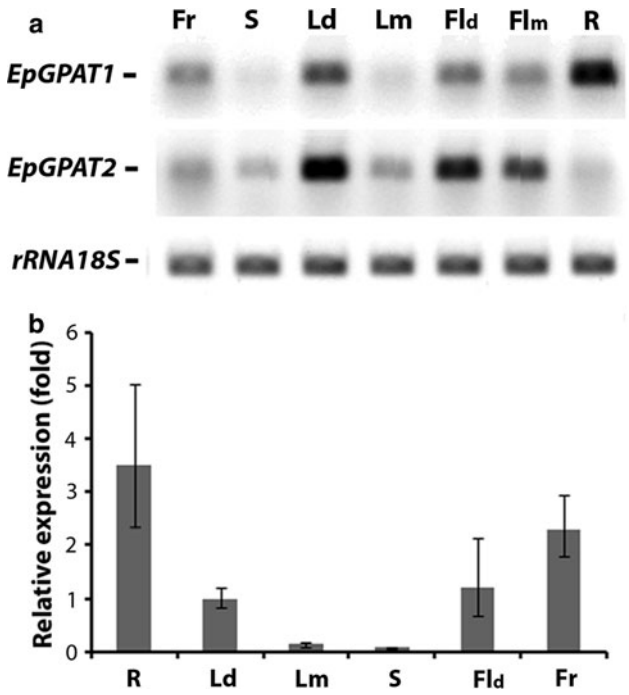

Fig. 3 Expression of *EpGPAT1* in different organs of *E. pitardii*. **a** Semi-quantitative RT-PCR assay. Equivalent cDNA amounts from different *Echium* organs: roots (*R*), young (*Ld*) or mature (*Lm*) leaves, stem (*S*), developing (*Fld*) or mature flowers at anthesis (*Flm*), and fruits (*Fr*), were subjected to PCR, using gene-specific primers for *EpGPAT1* and *EpGPAT2* (see "Materials and methods"). Identity of the PCR products was confirmed by direct sequencing of fragments. As a control for equal template loading, amplification of the rRNA18S was carried out. PCR samples were taken at cycle numbers determined to be non-saturating, 25 cycles for *EpGPAT* genes and 12 cycles for rRNA18S. PCR products were analyzed by 1.1% agarose gel electrophoresis and visualized by EtBr staining. **b** Quantitative PCR. cDNAs from organ samples shown above (except mature flowers) were analyzed by qPCR as described in "Materials and methods" using a TaqMan specific probe for *EpGPAT1* and the TaqMan Gene Expression Assay Eukaryotic 18S rRNA® (Applied Biosystems) as housekeeping. Expression levels are represented relative to that of the young leaf, besides standard deviation of the mean ($n = 5$)

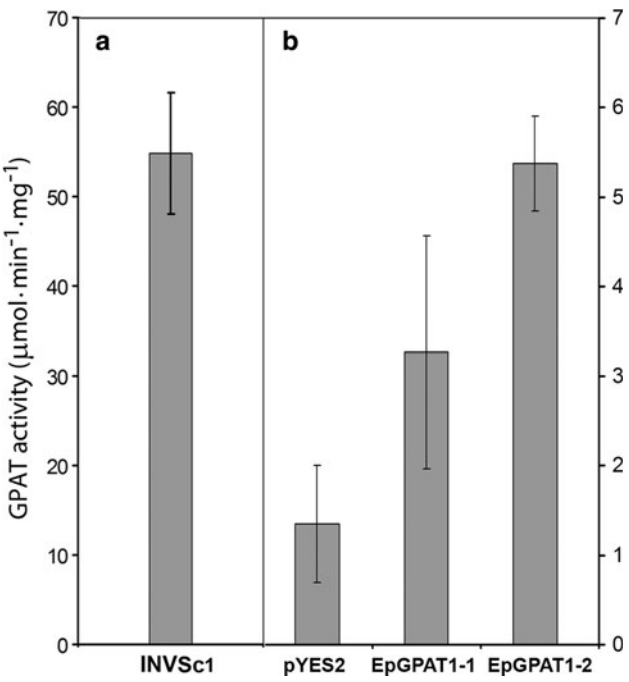

Fig. 4 GPAT activity of EpGPAT1-1 and EpGPAT1-2 measured by heterologous expression in yeast. **a** GPAT activity for the wild-type *INVSc1* yeast strain, used as a reference. **b** GPAT activity in particulate fractions of *gat-1*Δ mutants transformed with either the empty vector (*pYES2*) or the same plasmid containing the *EpGPAT1-1* and *EpGPAT1-2* genes. GPAT activity was measured on yeast cellular fractions obtained by sedimentation at 20,000 *g* for 30 min, and using oleoyl-CoA as a substrate (see "Materials and methods"). Data are expressed as average of three determinations besides the standard error of the mean

(Athenstaedt and Daum 1997). Consequently, we measured GPAT activity in a similar cellular fraction obtained by centrifugation at 20,000 *g* for 30 min (see "Materials and methods"). In all cases (wild-type and *gat1Δ* yeasts), this fraction contained about 90% of the total GPAT activity, while the remaining corresponded to the light microsomes fraction of the supernatant (results not shown). Two to four times increase in GPAT activity was obtained by overexpression of the two variants of *EpGPAT1*, relative to the level detected in the control with the pYES2 plasmid (Fig. 4). However, this is only one tenth, in the best case, of the activity recorded for the wild-type yeast INVSc1, thus indicating that the product of *EpGPAT1* has a low GPAT activity, at least under our assay conditions, as compared to the yeast endogenous GPATs.

The function of *EpGPAT1* was also investigated by overexpression of this gene in tobacco plants. The cDNAs for the two variants of *EpGPAT1* were cloned under the control of the constitutive 35S promoter from CaMV in the pBIN19 vector (Bevan 1984), and stable transformation with these constructs was achieved via *A. tumefaciens*. A total of 26 T_0 plants for *EpGPAT1-1* and 18 for *EpGPAT1-2* were obtained showing diverse expression of the transgenes, as determined by Northern-blot analysis, and plants transformed with the empty pBIN19 vector were used as a control in the experiments.

We did not register obvious phenotypic alterations in the *35S::EpGPAT1* transgenic plants. Given the high similarity of *EpGPAT* genes to *AtGPAT4/8* from *Arabidopsis* which have been involved in the biosynthesis of cutin polyesters (Li et al. 2007a), we have analyzed cutin monomer composition in leaves of tobacco plants overexpressing the *EpGPAT1* gene. A significant increase of the total monomer load was obtained for both variants of *EpGPAT1* (Fig. 5, inset). Major cutin components found in tobacco leaves are the C16:0 10,16 dihydroxy fatty acid and the C16:0 and C18:1 ω-hydroxyacids. All of

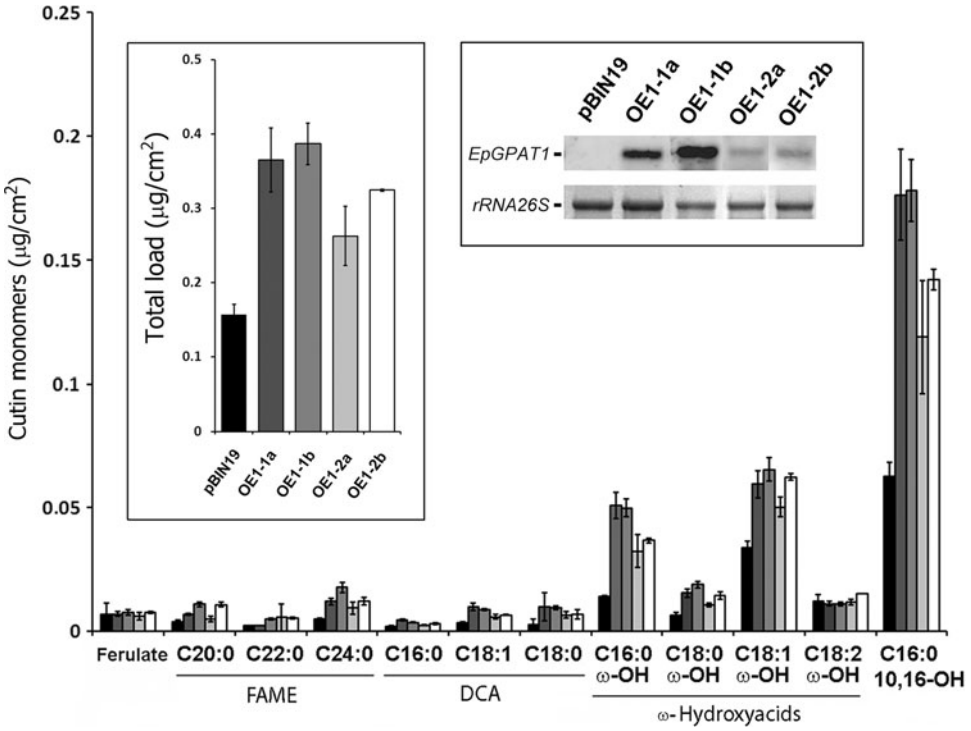

Fig. 5 Cutin monomer composition in leaves of transgenic *35S::EpGPAT1* tobacco plants. Leaf pools of T1 progeny plants from selected primary lines showing high expression of the *EpGPAT1-1* mRNA (*Northern-blot inset*) were analyzed. *OE1-1a* and *OE1-1b* correspond to plants transformed with *EpGPAT1-1*, while *OE1-2a* and *OE1-2b* are overexpressers of the *EpGPAT1-2* allelic variant. Total monomer loads are represented within the *left inset*. Mass values were normalized taking into account leaf areas and expressed as µg/cm^2. Data are means from three replicates with standard deviations shown. A significant difference (*t* test, two sided $P < 0.05$) was found for total increase in monomer load between vector control lines and that of transgenic lines. This include significant changes in *ω*-hydroxy fatty acid monomers (C16:0, C18:0, C18:1) and the major monomer 10,16 dihydroxy C16:0 fatty acids

them became significantly increased in *35S::EpGPAT1* plants, as well as most other minoritary cutin components (Fig. 5). This result is consistent with the increase in total cutin load observed in over-expressors of *AtGPAT4*, *8* or *6* (Li et al. 2007a; Li-Beisson et al. 2009). Similarly to what has been reported for *AtGPAT4/8*, overexpression of *EpGPAT1* does not have a remarkable effect on the wax fraction of the tobacco leaf (Supplementary Fig. 5a). Relative composition of individual hydrocarbons in this fraction was not substantially modified in *35S::EpGPAT1* plants (Supplementary Fig. 5b). Just some reduction of the anteiso alkanes a-30 and a-32 could be recorded, which is compatible with the notion of a common pool of acyl-CoAs in the epidermis for the synthesis of both cutins and wax, as previously reported (Li et al. 2007b). The load and composition of other major components of tobacco cuticular waxes such as, polyalcohols, diterpenes and sucrose esters (Severson et al. 1984) were also not significantly changed (Supplementary Fig. 5a).

To check for a possible role of *EpGPAT1* in the biosynthesis of membrane or reserve acyl-glycerolipids, analysis of fatty acids in tobacco leaves of *35S::EpGPAT1* transgenic plants was performed. Neither the total fatty acid content nor the fatty acid profile is significantly different to that of the control plants (results not shown).

Discussion

Involvement of GPAT-related enzymes in the biosynthesis of protective polymers, cutin and suberin, has been recently demonstrated in the model plant *A. thaliana* (Beisson et al. 2007; Li et al. 2007a, b; Li-Beisson et al. 2009). Data provided in this paper indicate that similar enzymes are also acting in *Echium* (Boraginaceae). Thus, two closely related genes (*EpGPAT1* and *EpGPAT2*) have been identified, likely representing *Echium* homologues of *Arabidopsis* genes involved in the synthesis of cutin. According to that notion, we have shown that 35S-driven expression of the *EpGPAT1* gene in tobacco plants increases cutin content in the leaves. This, together with biochemical data showing GPAT activity of the gene product, suggests that

EpGPAT1 catalyzes acyl transfer to a glycerol-based acceptor, similarly to what has been described for their *Arabidopsis* counterparts AtGPAT4 and AtGPAT8 (Li et al. 2007a). In a wider context, this finding also indicates that mechanisms leading to cutin biosynthesis are conserved among very diverse plant families, with the acyl transfer reaction operating as a rate limiting step.

Analysis of transcripts in different organs allowed us the detection of the two similar gene versions *EpGPAT1* and *EpGPAT2* in *Echium*. Strong similarity among *EpGPAT* genes (98.5% similarity for encoded proteins), and analysis of their expression patterns suggests that they may encode isozymes with distinct contributions along different plant tissues. Differential expression is more apparent in the roots, for instance, where the transcript for *EpGPAT1* is much more abundant than for *EpGPAT2*. This situation reminds to that reported for the pair *AtGPAT4*/*AtGPAT8*, which are also proteins sharing a high similarity (97.6%). In this case, the mRNA for *AtGPAT4* predominates in the roots over that of *AtGPAT8*. Conversely, similar expression of both genes is found in other parts of the plant such as the leaves, as in the case of *EpGPAT* genes. Despite this parallelism, phylogenetic analysis (Fig. 2) indicates that neither *EpGPAT1* and *AtGPAT4*, nor the pair *EpGPAT2* and *AtGPAT8* represent orthologues, since both *EpGPAT* genes appear as sister to the clade including the *Arabidopsis* genes. Therefore, it seems that gene duplication leading to isozyme pairs occurred independently in both groups of plants, after divergence from the Brassicaceae–Boraginaceae ancestor. This is intriguing given that *Arabidopsis* genes seem to play redundant functions in the plant, as indicated by the fact that only the double mutants exhibit phenotypic alterations (Li et al. 2007a). It is possible that differences among isozyme functions are more subtle. Anyway, with the available information it is not possible to ascertain if members of the AtGPAT4/EpGPAT1 and AtGPAT8/EpGPAT2 pairs perform similar functions in the plant, though this remains as an interesting possibility. We have also shown that expression of *EpGPAT1* and *EpGPAT2* seems to be higher in young tissues, such as developing leaves, than in older ones. This is in agreement to previous observations where a more active cutin biosynthesis has been reported in fast growing tissues (Hoffmann-Benning and Kende 1994; Viougeas and Chamel 1994).

Sequence analysis reveal that EpGPATs as well as AtGPAT4/AtGPAT8 counterparts, contain a N-terminal HAD-like domain attached to the acyltransferase moiety. The HAD domain is widespread over the three superkingdoms and is found in very diverse enzymes bearing hydrolytic activities. Small phosphorylated compounds such as sugars, aminoacids and nucleotides are among the typical substrates of HAD-like enzymes. Maximum homology of the HAD domain from GPATs out of plants is attained for members of the "PSP/P5N-1 assemblage" (Burroughs et al. 2006), which are characterized by the presence of a C1-type cap module with a four helix arrange. This group includes enzymes with diverse activities such as phosphoserine phosphatases (PSP family) and nucleotidases (P5N-1 familly). The presence of this typical hydrolytic domain in plant GPATs allows us to speculate with the possibility that GPAT enzymes behave as bifunctional enzymes catalyzing dephosphorylation of glycerol besides acyl transfer, thus yielding monoacylglycerols (MAGs) as the reaction product. It is interesting to note that accumulation of MAGs in leaf waxes is produced by overexpression of *AtGPAT5* both in *Arabidopsis* and in tobacco plants (Li et al. 2007b). While preparing this manuscript, we have known that AtGPAT4/AtGPAT6 certainly possess phosphatase activity (Yang et al. 2010). This confirmed our prediction from the HAD domain. It is interesting to notice that the HAD domain seems to be only present in the group of plant GPATs which have been involved in the synthesis of polyesters. Though the GPAT enzyme involved in the synthesis of soluble glycerolipids has not been yet identified in plants (out of plastids), GPATs from bacteria, yeast and animals do not contain the HAD motif. Therefore, it seems likely that attachment of the HAD domain to the acyltransferase moiety has uniquely evolved in plants to confer to these enzymes a distinct role in the biosynthesis of polymers that build protective surfaces.

Acknowledgments This work was supported by grants from the Ministerio de Ciencia y Tecnología (MCYT, AGL2005-01498/AGR) and Junta de Andalucía (P05-189-AGR). A. Mañas-Fernández was recipient of a postgraduate fellowship from the Junta de Andalucía.

References

Athenstaedt K, Daum G (1997) Biosynthesis of phosphatidic acid in lipid particles and endoplasmic reticulum of *Saccharomyces cerevisiae*. J Bacteriol 179:7611–7616

Bafor M, Stobart AK, Stymne S (1990) Properties of the glycerol acylating enzymes in microsomal preparations from the developing seeds of safflower (*Carthamus tinctorius*) and turnip rape (*Brassica campestris*) and their ability to assemble cocoa-butter type fats. J Am Chem Soc 67:217–225

Beisson F, Li Y, Bonaventure G, Pollard M, Ohlrogge JB (2007) The acyltransferase GPAT5 is required for the synthesis of suberin in seed coat and root of *Arabidopsis*. Plant Cell 19:351–368

Bevan M (1984) Binary *Agrobacterium* vectors for plant transformation. Nucleic Acids Res 12:8711–8721

Bonaventure G, Beisson F, Ohlrogge J, Pollard M (2004) Analysis of the aliphatic monomer composition of polyesters associated with Arabidopsis epidermis: occurrence of octadeca-cis-6, cis-9-diene-1, 18-dioate as the major component. Plant J 40:920–930

Bradford MM (1976) A rapid and sensitive method for the quantitation of microgram quantities of protein utilizing the principle of protein-dye binding. Anal Biochem 72:248–254

Burroughs AM, Allen KN, Dunaway-Mariano D, Aravind L (2006) Evolutionary genomics of the HAD superfamily: understanding the structural adaptations and catalytic diversity in a superfamily of phosphoesterases and allied enzymes. J Mol Biol 361: 1003–1034

Chang S, Puryear J, Cairney J (1993) A simple and efficient method for isolating RNA from pine trees. Plant Mol Biol Rep 11:113–116

Elble R (1992) A simple and efficient procedure for transformation of yeasts. BioTechniques 13:18–20

Franke R, Schreiber L (2007) Suberin—a biopolyester forming apoplastic plant interfaces. Curr Opin Plant Biol 10:252–259

Franke R, Briesen I, Wojciechowski T, Faust A, Yephremov A, Nawrath C, Schreiber L (2005) Apoplastic polyesters in *Arabidopsis* surface tissues—a typical suberin and a particular cutin. Phytochemistry 66:2643–2658

García-Maroto F, Garrido-Cárdenas JA, Rodriguez-Ruiz J, Vilches-Ferrón M, Adams AC, Polaina J, López-Alonso D (2002) Cloning and molecular characterization of the Δ^6-desaturase from two *Echium* plant species: production of γ-linolenic acid by heterologous expression in yeast and tobacco. Lipids 37:417–426

Graça J, Pereira H (2000) Methanolysis of bark suberins: analysis of glycerol and acid monomers. Phytochem Anal 11:45–51

Graça J, Schreiber L, Rodrigues J, Pereira H (2002) Glycerol and glyceryl esters of omega-hydroxyacids in cutins. Phytochemistry 61:205–215

Guerineau F (1995) Tools for expressing foreign genes in plants. Methods Mol Biol 49:1–32

Hoffmann-Benning S, Kende H (1994) Cuticle biosynthesis in rapidly growing internodes of deepwater rice. Plant Physiol 104: 719–723

Horsch RB, Fry JE, Hoffmann NL, Eichholtz D, Rogers SG, Fraley RT (1985) A simple and general-method for transferring genes into plants. Science 227:1229–1231

Kolattukudy PE (2001) Polyesters in higher plants. Adv Biochem Eng Biotechnol 71:1–49

Kunst L, Samuels AL (2003) Biosynthesis and secretion of plant cuticular wax. Prog Lipid Res 42:51–80

Kunst L, Samuels AL, Jetter R (2004) The plant cuticle: formation and structure of epidermal surfaces. In: Murphy DJ (ed) Plant lipids—biology, utilisation and manipulation. Blackwell Publishing, Oxford, pp 270–302

Lewin TM, Wang P, Coleman RA (1999) Analysis of amino acid motifs diagnostic for the sn-glycerol-3-phosphate acyltransferase reaction. Biochemistry 38:5764–5771

Li Y, Beisson F (2009) The biosynthesis of cutin and suberin as an alternative source of enzymes for the production of bio-based chemicals and materials. Biochimie 91:685–691

Li Y, Beisson F, Koo AJ, Molina I, Pollard M, Ohlrogge J (2007a) Identification of acyltransferases required for cutin biosynthesis and production of cutin with suberin-like monomers. Proc Natl Acad Sci USA 104:18339–18344

Li Y, Beisson F, Ohlrogge J, Pollard M (2007b) Monoacylglycerols are components of root waxes and can be produced in the aerial cuticle by ectopic expression of a suberin-associated acyltransferase. Plant Physiol 144:1267–1277

Li-Beisson Y, Pollard M, Sauveplane V, Pinot F, Ohlrogge J, Beisson F (2009) Nanoridges that characterize the surface morphology of flowers require the synthesis of cutin polyester. Proc Natl Acad Sci USA 106:22008–22013

Li-Beisson Y, Shorrosh B, Beisson F, Andersson M, Arondel V, Bates P, Baud S, Bird D, DeBono A, Durrett T, Franke R, Graham I, Katayama K, Kelly A, Larson T, Markham J, Miquel M, Molina I, Nishida I, Rowland O, Samuels L, Schmid K, Wada H, Welti R, Xu C, Zallot R, Ohlrogge J (2010) Acyl lipid metabolism. In: Last R (ed) The Arabidopsis book. American Society of Plant Biologists, Rockville. doi:10.1199/tab.0133

Livak KJ, Schmittgen TD (2001) Analysis of relative gene expression data using real-time quantitative PCR and the $2_T^{-\Delta\Delta C}$ Method. Methods 25:402–408

Mañas-Fernández A, Vilches-Ferrón M, Garrido-Cárdenas JA, Belarbi EH, Alonso DL, García-Maroto F (2009) Cloning and molecular characterization of the acyl CoA:diacylglycerol acyltransferase 1 (DGAT1) gene from *Echium*. Lipids 44:555–568

Moire L, Schmutz A, Buchala A, Yan B, Stark RE, Ryser U (1999) Glycerol is a suberin monomer. New experimental evidence for an old hypothesis. Plant Physiol 119:1137–1146

Molina I, Bonaventure G, Ohlrogge J, Pollard M (2006) The lipid polyester composition of *Arabidopsis thaliana* and *Brassica napus* seeds. Phytochemistry 67:2597–2610

Nawrath C (2002) The biopolymers cutin and suberin. In: Somerville C, Meyerowitz EM (eds) The Arabidopsis book. American Society of Plant Biologists, Rockville. doi:10.1199/tab.0021

Pollard M, Beisson F, Li Y, Ohlrogge JB (2008) Building lipid barriers: biosynthesis of cutin and suberin. Trends Plant Sci 13:236–246

Rodriguez-Ruiz J, Belarbi EH, Sanchez JLG, Alonso DL (1998) Rapid simultaneous lipid extraction and transesterification for fatty acid analyses. Biotechnol Tech 12:689–691

Rzhetsky A, Nei M (1992) Statistical properties of the ordinary least-squares, generalized least-squares, and minimum-evolution methods of phylogenetic inference. J Mol Evol 35:367–375

Severson RF, Arrendale RF, Chortyk OT, Johnson AW, Jackson DM, Gwynn GR, Chaplin JF, Stephenson MG (1984) Quantitation of the major cuticular components from green leaf of different tobacco types. J Agric Food Chem 32:566–570

Tamura K, Dudley J, Nei M, Kumar S (2007) MEGA4: Molecular Evolutionary Genetics Analysis (MEGA) software version 4.0. Mol Biol Evol 24:1596–1599

Taylor B, Powel A (1982) Isolation of plant DNA and RNA. Focus 4:4–6

Viougeas MA, Chamel A (1994) Radiolabelling studies of isolated leaf cuticles after in vivo incorporation of [^{14}C]acetate precursor in ivy plants. Plant Physiol Biochem 32:711–716

Yang W, Pollard M, Li-Beisson Y, Beisson F, Feig M, Ohlrogge J (2010) A distinct type of glycerol-3-phosphate acyltransferase with sn-2 preference and phosphatase activity producing 2-monoacylglycerol. Proc Natl Acad Sci USA 107:12040–12045

Zheng Z, Zou J (2001) The initial step of the glycerolipid pathway: identification of glycerol 3-phosphate/dihydroxyacetone phosphate dual substrate acyltransferases in *Saccharomyces cerevisiae*. J Biol Chem 276:41710–41716

Zheng Z, Xia Q, Dauk M, Shen W, Selvaraj G, Zou J (2003) *Arabidopsis AtGPAT1*, a member of the membrane-bound glycerol-3-phosphate acyltransferase gene family, is essential for tapetum differentiation and male fertility. Plant Cell 15:1872–1887

Zinser E, Sperka-Gottlieb CD, Fasch EV, Kohlwein SD, Paltauf F, Daum G (1991) Phospholipid synthesis and lipid composition of subcellular membranes in the unicellular eukaryote *Saccharomyces cerevisiae*. J Bacteriol 173:2026–2034